Diffusion Flame at High Pressure with Air and Water-laden Methane

Albert Jordà Juanós and William A. Sirignano
University of California, Irvine
Irvine, California, U.S.A.

1 Introduction

Water-laden combustion at high pressure is gaining interest for different applications, including rocket engines, methane hydrates, exhaust gas recirculation in engines, and bio-fuels. A counterflow canonical configuration is studied to obtain numerical results in relation to these applications. The paper is divided into two main sections: a gas-phase study, and a two-phase shifting equilibrium analysis. The former part provides results for a diffusion flame where the fuel stream contains a varying amount of water vapor. The latter part describes the shifting equilibrium formulation that must be coupled with a physical model when two phases are considered. In the presentation, results of this coupling with the counterflow diffusion flame problem will be discussed.

2 Gas-Phase Water-Laden Counterflow

We analyze different mixtures of methane and water vapor in a jet impinging against an air jet. Results are obtained at pressures ranging from 1 to 100 atm. The one-dimensional similar model for laminar counterflow diffusion flames is used with modifications in the energy equation to account for the proper evaluation of the mixture enthalpy at high densities. Real-gas effects are taken into account with the use of the Soave-Redlich-Kwong cubic equation of state. The model is equipped with a detailed reaction mechanism (GRI 3.0) and detailed transport properties are also evaluated for real gases. The governing equations are discretized using second-order finite difference schemes for non-uniform grids. Solutions are obtained using a modified Newton's iterative method. The grid is initially coarse and is progressively refined in the regions with steepest gradients to achieve mesh independence. Absolute and relative convergence tolerances are defined to be less or equal to 10^{-6} and 10^{-3}, respectively. The reader is referred to [1] for details related to the mathematical model and numerical method. The distance between the two nozzles is fixed to 2 cm. The velocity at the exit of the fuel nozzle is 1 m/s. The velocity at the exit of the oxidizer nozzle is such that the mass fluxes match between the two streams. The temperature of the inflowing air is 300 K, while it equals 600 K for the mixture of methane and water vapor to prevent the existence of a condensed phase. Analysis

Correspondence to: ajordaju@uci.edu

in [1] shows that, for the centimeter scale considered here, radiative transport, turbulence generation, and the Soret effect are negligible in the flame region, even at the highest pressure considered.

Three cases are studied with increasing amounts of water vapor in the fuel stream: 10%, 20% and 40%. For brevity, only a few representative plots are reported for the last case in figure 1. The plots for the 10% and 20% water fraction cases can be found elsewhere [2]. The trends with increasing water content are discussed below.

At 10% water vapor, temperature profiles highlight that raising pressure increases flame temperature, narrows flame width, and the temperature peak moves closer to the stagnation plane. Flame temperature at 1 atm is 2,029 K while it equals 2,305 K at 100 atm. These values are 42 K and 49 K hotter than for a case with 0% water, respectively, where the inflowing temperature equals 300 K for both nozzles. Note that the temperature boundary condition on the left side is 300 K greater when water is included in the fuel stream. Thus, a simulation where the left temperature matches the 600 K boundary condition is performed. The resulting flame temperature at 1 atm is 2,043 K. The flame temperature becomes 14 K colder at 1 atm when 10% water is included, indicating that water acts as an energy sink. Nevertheless, 14 K is not a very substantial temperature difference.

The presence of water, which is heavier than methane, tends to increase the density on the fuel side when the water fraction is increased from 0 to 10% if temperature is kept constant. However, we increased the temperature on the fuel-nozzle boundary, and density is more sensitive to the temperature change, resulting in a density decrease. Regarding the compressibility factor, the trend is inverted on the fuel side with respect to a case with no water. Here the effect of the compressibility factor Z with increasing pressure also contributes to reduce density.

Water product is generated in the flame region, where its mass fraction becomes greater than at the boundary for all pressures. The peak value increases with pressure and the region where it is generated narrows down consistently with the flame thickness. CO_2 production does not seem to be altered with the presence of extra water.

Dynamic viscosity and thermal conductivity (μ and λ) are more sensitive to temperature changes than they are to an increased amount of water vapor in the fuel stream. Thus, both these properties are not altered with respect to the case with 0% water.

When the water content in the fuel mixture is elevated to 20%, the flame temperature is 21 K colder at 1 atm and 31 K colder at 100 atm compared to the 10% water case. These flame temperatures are also lower than the case with no water. Again, the energy sink effect of water is dominant, and the consequence is even lower flame temperatures when more water is added. Density remains practically unaltered with respect to the 10% case. The presence of more water content on the fuel side of the domain affects the compressibility factor $Z = p/(\rho RT)$ where all the $(1 - Z)$ curves are moved in the positive direction, tending to increase the density ρ of the mixture. The presence of higher water vapor in the fuel stream increases the magnitude of the enthalpy departure function keeping the same sign in the cold zone on the fuel side. In the heat-release zone, the enthalpy departure behaves as in the case with 10% water.

Mass fraction of water features a local peak in the flame region, where more water is generated as a combustion product, but its magnitude now is lower than the 0.2 value at the fuel nozzle boundary. No changes occur in the CO_2 mass fraction. Transport properties are also not altered.

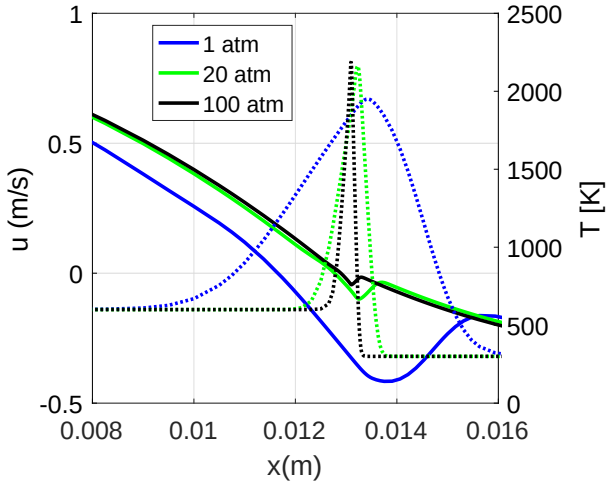

(a) Solid: u, Dotted: T

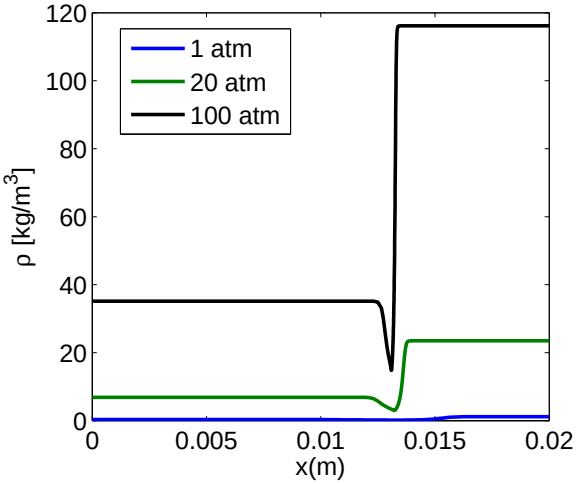

(b) ρ

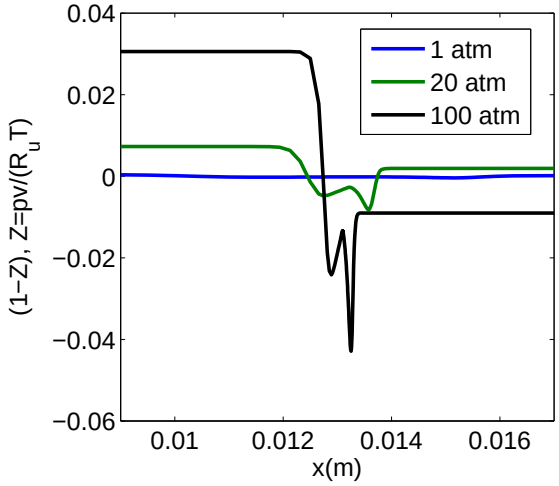

(c) $1 - Z$

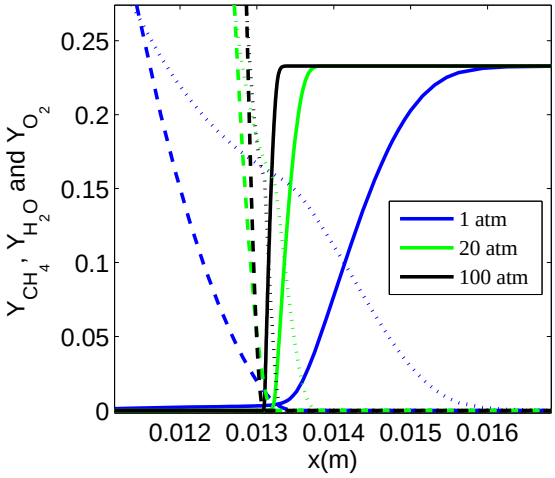

(d) Dashed:$Y_{\mathrm{CH_4}}$, Dots:$Y_{\mathrm{H_2O}}$, Solid:$Y_{\mathrm{O_2}}$

Figure 1: Set of solutions with 40% water vapor in the fuel stream.

Figure 1 contains the solutions for the case in which water vapor in the fuel stream is 40%. Similarly to all previous cases, the stagnation plane lies to the right of the symmetry plane. Peak temperature at 1 atm is 56 K colder compared to the case with 20% water, and it is 90 K colder at 100 atm. Density is shown in sub-figure 1b, portraying a slight increase with respect to the case with 20% water on the cold fuel stream region. The $1 - Z$ trend discussed for 20% water is even more obvious here as shown in sub-figure 1c, where all the curves are now positive at the fuel nozzle boundary.

Methane, oxygen, and water mass fractions are represented in Figure 1d. The water mass fraction flowing from the left is now too high compared to the water generated as a combustion product. This translates into a smooth decrease of the mass fraction gradient in the flame zone, which becomes steep again for greater x. The local peak that was identified in the cases with 10 and 20% water no longer exists. The enthalpy departure function becomes more significant in the cold region of the fuel side, while it is diminished within the flame zone. Transport properties remain unaffected.

The water content in the fuel stream was increased above 40% with the goal of finding the burning limit. The greatest percentage of H_2O resulting in a flame solution is 67% at 1 atm, with a flame temperature of 1,607 K. Further study of this limit is required, including results at high pressure.

3 Two-Phase Shifting Equilibrium

A gaseous mixture of methane and water vapor was considered in the previous section for the diffusion flame. In this second part, we consider a two-phase mixture on the fuel side of the counterflow where the gas and liquid contain the same two components in phase equilibrium. Part of the liquid water will vaporize into the gas, and some of the gaseous methane will dissolve into the liquid. The mole fractions of either component can be determined in each phase according to the high-pressure phase equilibrium formulation. It is described in [3], and solutions for different binary and multicomponent mixtures were reported.

As the two-phase mixture is advected towards the flame, heat is conducted from the reaction zone and the liquid completely vaporizes. There is a narrow region in which the two-phase mixture receives heat from combustion in the gas phase occurring in the vicinity of the phase-change location. There, we analyze the case where a shift in the species mass fractions and density is caused by a temperature change.

With only phase change and no chemical change, N_i (the number of moles of species i) remains fixed at its initial value N_{i0}; that is $N_{gi} + N_{li} = N_i = N_{i0} = constant$. Defining the mole number of the gas mixture as $N_g = \sum_{i=1}^{K} N_{gi}$ and the mole number of the liquid mixture as $N_l = \sum_{i=1}^{K} N_{li}$, where K is the total number of species, we also have $N_g + N_l = N = N_0 = constant$. With this, it is convenient to express the mole fractions normalized over both phases. Let $\xi_g \equiv N_g/N_0$; $\xi_l \equiv N_l/N_0$; $\xi_{gi} \equiv N_{gi}/N_0$; and $\xi_{li} \equiv N_{li}/N_0$. Their relation with the common mole fractions are

$$\xi_{gi} = X_{gi}N_g/N_0 = X_{gi}\xi_g;\ \xi_{li} = X_{li}N_l/N_0 = X_{li}\xi_l;\ X_{gi} = \xi_{gi}/\xi_g;\ X_{li} = \xi_{li}/\xi_l;\ i = 1, ..., K-1 \quad (1)$$

Consequently,

$$\xi_{gi} + \xi_{li} = \frac{N_{i0}}{N_0} = \xi_i = \xi_{i0};\ i = 1, ..., K \quad (2)$$

At equilibrium between the multicomponent gas and the liquid solution, the pressure p, temperature T, species chemical potential μ_i, and species fugacity f_i are continuous across the phase interface. The phase

equilibrium conditions for each species i is given by the following relations between the species fugacity coefficients in the two phases:

$$X_{li}\Phi_{li} = X_{gi}\Phi_{gi};\ i = 1, ..., K \tag{3}$$

where

$$\sum_{i=1}^{K} X_{li} = 1;\ \sum_{i=1}^{K} X_{gi} = 1 \tag{4}$$

There are K species and K phase-equilibrium relations. Taking changes in Equation 3 due to pressure and temperature, and differentiating the mole fraction definitions provided above, we can obtain a system of equations governing the shifting equilibrium. We define $A_i \equiv [\beta_{ik}]^{-1}[\delta_k]$ and $B_i \equiv [\beta_{ik}]^{-1}[\epsilon_k]$:

$$\begin{aligned}
&d\xi_{gi} = -d\xi_{li} = A_i dp + B_i dT;\\
&dX_{li} = [\frac{X_{li}\sum_{j=1}^{K} A_j - A_i}{\xi_l}]dp + [\frac{X_{li}\sum_{j=1}^{K} B_j - B_i}{\xi_l}]dT;\\
&dX_{gi} = [\frac{X_{li}\sum_{j=1}^{K} A_j - A_i}{\xi_g}]dp + [\frac{X_{li}\sum_{j=1}^{K} B_j - B_i}{\xi_g}]dT;\\
&i = 1, ..., K
\end{aligned} \tag{5}$$

Heat can be added to an element of mass of the two-phase mixture due to heat transferred from the reacting zone. The liquid phase will disappear due to vaporization before the mass reaches the flame. Assume a small amount of heat per unit mole dQ is added to the mixture at constant pressure:

$$dh = \xi_g(dh_g - dh_l) + dh_l + (h_g - h_l)d\xi_g = dQ \tag{6}$$

The differential of enthalpy per unit mole for a multi-component gas or liquid is given as

$$dh = \left(\frac{\partial(h - h^*)}{\partial T}\ |_{p,X_i} + \frac{\partial h^*}{\partial T}\ |_{X_i}\right) dT + \sum_{i=1}^{K}\left(\frac{\partial(h - h^*)}{\partial X_i}\ |_{p,T,X_j,j\neq i} + \frac{\partial h^*}{\partial X_i}\ |_{T,X_j,j\neq i}\right) dX_i \tag{7}$$

Through Equations 6 and 7, the added heat dQ causes a change dT in the temperature. The change in the temperature causes a shift in X_{gi}, X_{li}, ξ_{gi}, and ξ_{li} through Equations 5.

These equations can be used to consider a flow where methane and water flow together with two phases at the same temperature. One phase is a gas with methane and water vapor. The other phase has liquid water with dissolved methane. The above equations can be recast to give moles per unit volume (or mass per unit volume) and coupled with the energy equation. Results on the shifting equilibrium problem are expected over the next month to be included in the oral presentation.

3 Conclusion

A counterflow diffusion flame configuration has been used to obtain numerical results for a fuel jet impinging against air for high pressures up to 100 atm. The first part of the paper studies the gas-phase problem, where different fractions of water vapor are mixed with the methane in the fuel stream. The trends in flame temperature, mass fractions, density, and compressibility factor have been discussed when the mole fraction of water vapor is 10%, 20%, and 40%. The main effect on the flame is a reduction of its peak temperature

with increasing water content. The effects on flame structure are not altered with respect to those induced by increments in pressure. The peak in water mass fraction that appears within the reaction zone at low water contents disappears when enough water is added with the fuel. Transport properties are enhanced with increasing water content, with no substantial effect on the flame.

The second part of this study introduces the shifting equilibrium formulation to be implemented when the two-phase problem is considered. In this scenario, gaseous methane dissolves in the liquid and a fraction of water vaporizes in the gas phase. As this mixture is advected towards the flame, there is a narrow region where it experiences variations in mole fractions and density under a shifting equilibrium process controlled by the heat conducted from the gaseous region where combustion takes place.

References

[1] A. Jordà Juanós and W. A. Sirignano, "Pressure effects on real-gas laminar counterflow," *Combust. Flame*, vol. 181, pp. 54–70, 2017.

[2] A. Jordà Juanós and W. A. Sirignano, "Counterflow analysis for combustion at high pressure," in *AIAA SciTech 2016, Aerospace Sciences Meeting*, no. AIAA-2016-0445. San Diego, CA: AIAA, 2016.

[3] A. Jordà Juanós and W. A. Sirignano, "Thermodynamic analysis for combustion at high gas densities," in *Proceedings of the 25th ICDERS*. Leeds, UK: ICDERS, 2015.